Journal of Fluorescence, Vol. 6, No. 4, 1996

Distance-Dependent Quenching of Nile Blue Fluorescence by *N,N*-Diethylaniline Observed by Frequency-Domain Fluorometry

Joseph R. Lakowicz,[1] Bogumil Zelent,[1] Józef Kuśba,[1] and Ignacy Gryczynski[1]

Received January 16, 1996; accepted August 7, 1996

Fluorescence quenching of Nile Blue by amines is thought to be due to electron transfer to the excited dye molecule from the amine electron donor. We used electron transfer quenching of Nile blue by *N,N*-diethylaniline in propylene glycol as a model system for an interaction which depends exponentially on distance. We investigated the time dependence of the presumed distance-dependent process using gigahertz harmonic-content frequency-domain fluorometry. The frequency-domain data and the steady-state quantum yield were analyzed globally based on either the Smoluchowski–Collins–Kimball radiation boundary condition (RBC) model or the distance-dependent quenching (DDQ) model, in which the rate of quenching depends exponentially on the flourophore–quencher distance. We performed a global analysis which included both the frequency-domain time-resolved decays and the steady-state intensities. The latter were found to be particularly sensitive to the model and parameter values. The data cannot be satisfactorily analyzed using the RBC model for quenching. The analysis shows the excellent agreement of the DDQ model with the experimental data, supporting the applicability of the DDQ model to describe the quenching by the electron transfer process, which depends exponentially on the donor–acceptor distance.

KEY WORDS: Fluorescence; quenching; electron transfer; time-resolved fluorescence; frequency-domain fluorometry.

INTRODUCTION

Photo-induced electron transfer is the primary photoreaction process of interest in many aspects of chemistry[1–3] and biochemistry.[3–6] To study further the process of electron transfer, we examined quenching of fluorescence under conditions in which electron transfer can be expected to occur. Excited-state electron transfer has been studied extensively by Weller and co-workers.[7,8] The efficiency of the electron transfer in a donor (D)–acceptor (A) system, when one of the molecules is in the excited electronic state, is characterized by the free energy change (ΔG_{ET}) of the quenching process,

$$\begin{matrix} D^* & + & A & \searrow & \\ & & & & (D^+ \cdots A^-)_s \xrightarrow{\text{polar solvent}} D_s^+ + A_s^- \\ D & + & A^* & \nearrow & \end{matrix}$$

The free energy change of the electron transfer quenching is expressed by the equation

$$\Delta G_{ET} = E_{1/2}^{0X}(D/D^{+}\cdot) - E_{1/2}^{red}(A^{-}\cdot/A) - E^* + C \quad (1)$$

$E_{1/2}^{OX}(D/D^+)$ and $E_{1/2}^{red}(A^-\cdot/A)$ refer to the half-wave oxidation potential of the electron donor and reduction potential of the electron acceptor, respectively.[7,8] E^* is the electronic excitation energy of the excited molecule. In this expression, C refers to the Coulomb energy change associated with the charge separation distance R,[9] expressed as $C(\text{eV}) = -e^2/\varepsilon R 4\pi\varepsilon_0$, where e is the electronic charge, ε is the static dielectric constant of a

[1] Center for Fluorescence Spectroscopy, Department of Biological Chemistry, University of Maryland at Baltimore, School of Medicine, 108 North Greene Street, Baltimore, Maryland 21201.

1053-0509/96/1200-0187$09.50/0

solvent, and ε_0 is the permittivity constant. Rehm and Weller[7,8] also showed that the rate constant, k_q, of the electron transfer quenching is related to the free energy ΔG_{ET}. This relation was experimentally determined for many aromatic fluorophores quenched by typical electron donors.[1,2,7,8]

Since the classical work of Weller and his co-workers, a number of reports have indicated that the rate constant, k_q, apart from the free energy change, is also controlled by the donor–acceptor distance, the polarity of the solvent, the dynamic properties of the solvent, and the temperature.[10–14] Hence we studied collision quenching of fluorescence in order to determine the effects of distance to the rates of electron transfer quenching. Heteroaromatic dyes like coumarins,[15] oxazine,[16] and Nile Blue[16–19] have been found to be good electron acceptors and their fluorescence can be quenched by aromatic amines on a femtosecond time scale.[15–19] Ultrafast electron transfer between the excited dye molecules and aniline or *N,N*-dimethylaniline has been studied to reveal the effect of solvent and intramolecular dynamics on the reaction. Among these dyes, we chose Nile Blue as an interesting cationic fluorophore which can be collisionally quenched by an electron transfer process in the presence of diffusion and, thus, serve as a model for distance-dependent collisional quenching. Fluorescence quenching of Nile Blue by *N,N*-diethylaniline in propylene glycol was studied by frequency-domain fluorometry and steady-state measurements. The results were analyzed using the radiation boundary condition (RBC) model,[20,21] which assumes a single rate of quenching at the encounter distance, and the distance-dependent quenching (DDQ) model,[22,23] which is thought to be suitable for electron transfer quenching.

THEORY

For the Smoluchowski–Collins–Kimball (RBC) model the quenching rate $k(r)$ assumes a value of $\kappa\ \delta(r - a)$ when the fluorophore and quencher are at the encounter distance a, which is the distance of the fluorophore–quencher closest approach, and the quenching rate is zero elsewhere. No specific form of the intermolecular interactions is involved in this model. For the exponential distance-dependent quenching (DDQ) model the expression for the rate of quenching can be written as

$$k(r) = k_a \exp\left(-\frac{r - a}{r_e}\right) \tag{2}$$

where r_e is the characteristic transfer distance, and k_a is the value of transfer rate at $r = a$. This dependence on distance is appropriate in electron transfer and exchange interactions.[10,24–29]

The influence of quenching on fluorophore intensity decay is given by

$$I(t) = I_0 \exp\left[-\frac{t}{\tau_0} - C_q \int_0^t k(t')\, dt'\right] \tag{3}$$

where τ_0 is the fluorophore lifetime without quenching, C_q^0 is the bulk concentration of the quencher, and $k(t)$ denotes the averaged time-dependent fluorophore–quencher reaction rate constant. The rate constant $k(t)$ can be expressed as

$$k(t) = \frac{4\pi}{C_q^0} \int_a^\infty r^2\, k(r)\, C_q(r,t)\, dr \tag{4}$$

where $C_q(r,t)$ is the concentration of the quencher molecules at distance r from the excited fluorophore at time instant t. In order to simplify the calculations, one introduces the function $y(r,t) = C_q(r,t)/C_q^0$. In the presence of diffusion the function $y(r,t)$ is governed by the diffusion equation. The equation has an additional sink term which is responsible for the through-space fluorescence quenching,

$$\frac{\partial y(r,t)}{\partial t} = D\nabla^2 y(r,t) - k(r)y(r,t) \tag{5}$$

where $D = D_F + D_Q$ is the mutual diffusion coefficient of the fluorophore and the quencher with diffusion coefficients D_F and D_Q, respectively. For both quenching models the initial and outer boundary conditions of Eq. (5) remain the same

$$y(r, t = 0) = 1 \tag{6}$$

$$\lim_{r\to\infty} y(r,t) = 1 \tag{7}$$

The form of the inner boundary condition (at $r = a$) depends on the particular model. For the RBC model we have

$$\left[\frac{\partial y(r,t)}{\partial r}\right]_{r=a} = \frac{\kappa}{D} y(r = a, t) \tag{8}$$

whereas for the DDQ model one assumes the "reflecting" or "specular" boundary condition at $r = a$

$$\left[\frac{\partial y(r,t)}{\partial r}\right]_{r=a} = 0 \tag{9}$$

This condition indicates that donor–quencher encounters

do not introduce any other deactivation channel apart from that described by the rate $k(r)$.

For the RBC model the diffusion Eq. (5) can be solved analytically.[30] For the DDQ model an exact analytical solution of the Eq. (5) is not possible, and numerical methods are required. In this paper we used an algorithm described previously[31,32] based on the numerical solution of the diffusion Eq. (5) in the Laplace space[33] and numerical integration of the Eq. (4).

Using the technique of frequency-domain fluorometry,[34,35] one compares the experimental phase (ϕ_ω) and modulation (m_ω) values with those calculated (c) from the model intensity decay $I(t)$. At a given modulation frequency (ω) these values are given by

$$\phi_{c\omega} = \arctan (N_\omega/D_\omega) \tag{10}$$

$$m_{c\omega} = \frac{1}{J}(N_\omega^2 + D_\omega^2)^{1/2} \tag{11}$$

where

$$N_\omega = \int_0^\infty I(t) \sin(\omega t)\, dt \tag{12}$$

$$D_\omega = \int_0^\infty I(t) \cos(\omega t)\, dt \tag{13}$$

$$J = \int_0^\infty I(t)\, dt \tag{14}$$

The fluorophore quantum yield is another experimental observable, which can also be predicted by the quenching models. In this paper we examined the Stern–Volmer-type quantity f defined as

$$f = \frac{F_0}{F} - 1 \tag{15}$$

where F_0 and F are fluorophore quantum yields in the absence and presence of quencher. The ratio F/F_0 constitutes the relative quantum yield of the fluorophore and may be calculated as

$$\frac{F}{F_0} = \frac{\int_0^\infty I(t)\, dt}{\int_0^\infty I^0(t)\, dt} \tag{16}$$

where $I(t)$ is expressed by Eq. (3) for either the RBC or the DDQ model and $I^0(t) = I_0\exp(-t/\tau_0)$ is the fluorophore's intensity decay in the absence of quencher.

MATERIALS AND METHODS

Nile Blue laser dye from Lambda Physik (Bedford, MA) was used without further purification. *N,N*-Diethylaniline (P.A. grade), from Fluka Chemie A.G. (Switzerland), was purified by vacuum distillation in a grease-free, mercury-free vacuum line. The colorless liquid aromatic amine was stored under an oxygen-free nitrogen atmosphere in the dark. The concentration of Nile Blue in the samples was 1.3×10^{-6} *M* using an extinction coefficient of 7.75×10^4 M^{-1} cm^{-1} at 633 nm in ethanol. The concentration of *N,N*-diethylaniline ranged from 0 to 0.3 *M*. The stock solution of *N,N*-diethylaniline (0.3125 *M*) in propylene glycol was purged by oxygen-free nitrogen gas and equilibrated for 24 h at room temperature in the dark. 1,2-Propanediol (propylene glycol) (P.A. grade) was from Janssen Chimica (Spectrum Chemical Mfg. Corp., Gardena, CA). Absorption spectra were measured on a Perkin–Elmer Lambda 6, UV/vis spectrophotometer (Perkin–Elmer Corporation, Rockville, MD). Steady-state fluorescence measurements were carried out using a SLM 8000 photon-counting spectrofluorometer (SLM Instruments, Inc., Urbana, IL) equipped with a thermostated cell holder.

The time-resolved frequency-domain fluorescence measurements were performed on a multifrequency phase-modulation spectrometer described in detail previously.[34,35] The excitation source was a 3.795-MHz train of pulses, about 7 ps wide, obtained from the cavity-dumped output of a synchronously pumped rhodamine-6G dye laser. The dye laser output was 600 nm. The dye laser was pumped with a mode-locked Nd:YAG laser, 2 W at 532 nm, FWHM = 100 ps. The fluorescence emission was detected using an MCP-PMT Hamamatsu R2809 red-sensitive detector, which was externally cross-correlated. All intensity decays were measured using rotation-free polarization conditions, with the fluorophore emission selected by an interference filter, 10-nm bandwidth at 660 nm (Ditric Optics, Inc., Hutson, MA). The frequency-domain data were collected and transferred to a Silicon Graphics Indy workstation for analysis.

The best-fit parameters and goodness-of-fit are determined by the minimum value of

$$\chi_R^2 = \frac{1}{\nu}\left[\sum_\omega \left(\frac{\phi_\omega - \phi_{c\omega}}{\delta\phi}\right)^2 + \sum_\omega \left(\frac{m_\omega - m_{c\omega}}{\delta m}\right)^2 + \sum_i \left(\frac{f_i - f_{ci}}{\delta f_i}\right)^2\right] \tag{17}$$

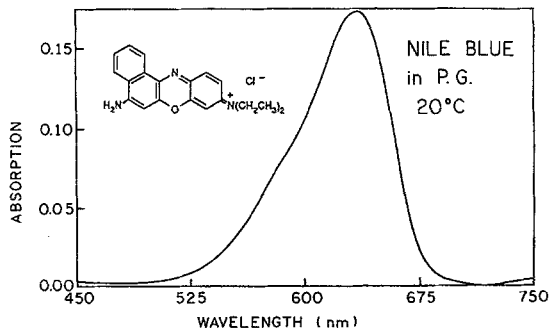

Fig. 1. Chemical structure of Nile Blue and its absorption spectrum in propylene glycol.

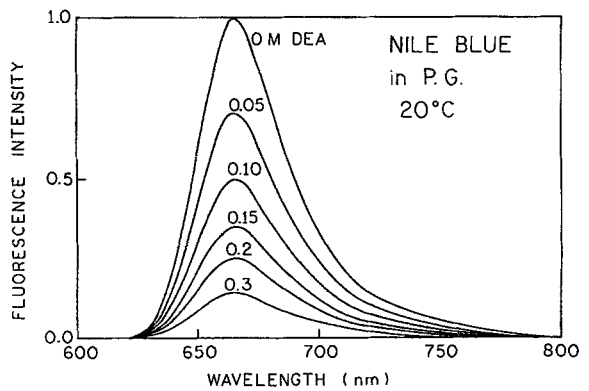

Fig. 2. Fluorescence emission spectra of Nile Blue in propylene glycol at 20°C (λ_{exc} = 620 nm) in the presence of increasing concentrations of *N,N*-diethylaniline (0, 0.05, 0.1, 0.15, 0.2, and 0.3 *M*).

where ν is the number of degrees of freedom and $\delta\phi$, δm, and δf are the experimental uncertainties. For all analyses, the uncertainties $\delta\phi$ and δm were taken as 0.2° in the phase angle and 0.005 in the modulation ratio, respectively. The uncertainties δf_i were calculated from the relation $\delta f_i = (F_0/F_i)^2 \times (\Delta F/F_0)$. We assume uncertainties of $\Delta F/F_0 = 0.005$ for Nile Blue quenched by *N,N*-diethylaniline in propylene glycol.

RESULTS AND DISCUSSION

Figure 1 shows the electronic absorption spectrum of Nile Blue (NB) in propylene glycol. The spectrum is characterized by the absorption band between 500 and 700 nm, with the maximum near 630 nm. We have observed that the shape and intensity of the absorption band of NB remain unchanged in the presence of 0.3 *M* *N,N*-diethylaniline (DEA). This indicates that no specific interactions exist between the dye and the aromatic

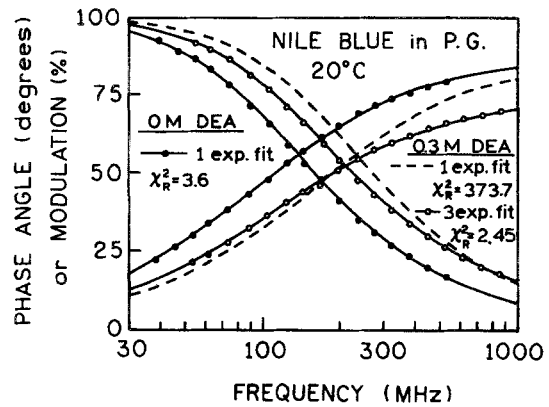

Fig. 3. Frequency response of the Nile Blue fluorescence intensity decay in propylene glycol at 20°C. The filled circles and solid line represent the data and best single-exponential fit in the absence of DEA. The open circles and solid line represent the data and best three-exponential fit with 0.3 *M* DEA. The dashed lines shows the best single-exponential fit to data with 0.3 *M* DEA.

amine molecules in the ground electronic state. However, the fluorescence of NB is quenched by DEA, indicating interactions between the singlet excited NB and DEA molecules. The fluorescence emission of NB in propylene glycol at 667 nm strongly decreases in intensity in the presence of increasing concentrations of DEA (see Fig. 2), without any change in the shape or appearance of new emissions. The observed quenching is reported due to electron transfer from DEA to the cationic dye NB.[16-18]

The electron transfer mechanism of fluorescence quenching of NB by DEA is due to the comparatively low ionization potential of DEA (7.15 eV,[36]) which is a typical electron donor molecule, and the fact that cationic dye NB can act as an electron acceptor. Also, DEA possesses a higher-lying excited-singlet state (4.10 eV) than the NB molecule (1.97 eV) in propylene glycol, preventing electronic energy transfer (Förster type) in this system. Quenching of NB by DEA is an interesting example of collisional quenching of fluorescence for which the dependence of the quenching rate constant on the fluorophore–quencher distance can be measured from the frequency-domain and steady-state data and the results compared with the expected distance dependence.

We used frequency-domain time-resolved measurements of the NB intensity decays to investigate the form of the quenching interaction. From previous studies, we knew that the Smoluchowski, RBC,[20,21] and DDQ[22,23] quenching models all resulted in distinct intensity decays. Figure 3 shows the frequency response of the intensity decay of NB in propylene glycol in the absence and presence of 0.3 *M* DEA. It is shown that experi-

Table I. *N,N*-Diethylaniline Quenching of Nile Blue in Propylene Glycol: Multiexponential Analysis of Fluorescence Intensity Decays at 20°C

C_Q (*M*)	τ_i (ns)	$\bar{\tau}$ (ns)	α_i[a]	f_i	χ^2_R 1 exp.	χ^2_R 2 exp.	χ^2_R 3 exp.
0	1.744	1.744	1.0	1.0	3.60	—	—
0.1	1.583	1.543	0.831	0.970	54.87	2.72	—
	0.243		0.169	0.030			
0.2	1.419	1.351	0.707	0.944	184.2	3.73	—
	0.204		0.293	0.056			
0.3	1.311	1.203	0.309	0.899	373.7	3.06	2.45
	0.289		0.131	0.084			
	0.014		0.560	0.017			

[a]The multiexponential decay is given by $I(t) = \Sigma_i\ \alpha_i \exp(-t/\tau_i)$, where α_i are the preexponential function and τ_i the decay times. The value of f_i are given by $f_i = \alpha_i\ \tau_i/\Sigma_j\ \alpha_j\ \tau_j$.

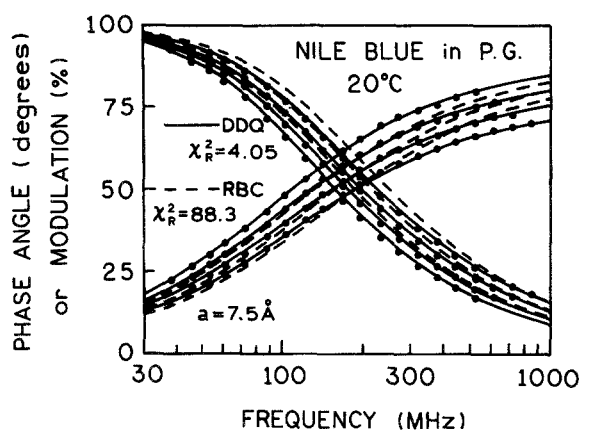

Fig. 4. Frequency-domain intensity decays of Nile Blue in propylene glycol in the presence (left to right) of increasing concentrations of *N,N*-diethylaniline (0, 0.1, 0.2, and 0.3 *M*). The solid lines and dashed lines show the best fit to the DDQ and the RBC model, respectively, using a = 7.5 Å.

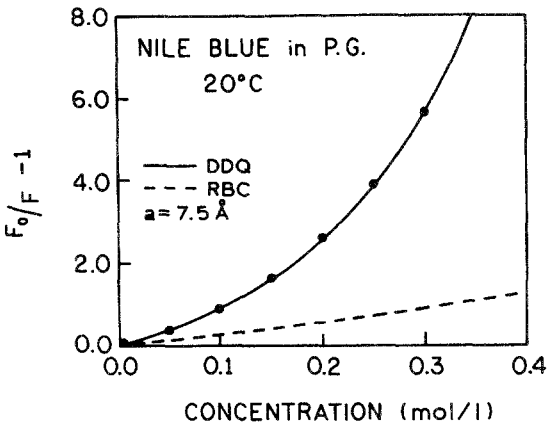

Fig. 5. Stern–Volmer plots for Nile Blue in propylene glycol at 20°C quenched by *N,N*-diethylaniline. The solid line represents the calculated values of $[(F_0/F) - 1]$ using the DDQ model, and the dashed line is for the best RBC analysis. The distance of the closest approach was held fixed at a = 7.5 Å during the analyses.

mental data points for NB in the absence of DEA (•) can be satisfactorily fitted using a monoexponential decay with τ_0 = 1.744 ns (χ^2_R = 3.60). Figure 3 shows that the intensity decays of NB become heterogeneous in the presence of DEA. In the presence of 0.3 *M* DEA the monoexponential decay (---) cannot fit the data (○), as can be judged by χ^2_R = 373.7. Three decay times are needed to fit the data. The multiexponential analysis yields τ_1 = 1.311 ns (α_1 = 0.309), τ_2 = 0.289 ns (α_2 = 0.131), and τ_3 = 0.014 ms (α_3 = 0.560) with χ^2_R = 2.45. When the concentration of DEA increases from 0 to 0.3 *M*, the fluorescence intensity decay of NB becomes increasingly heterogeneous, as can be seem from the χ^2_R values for the single-exponential fits in Table I. Quenching results in progressive shifting of the frequency response to higher frequencies with a corresponding decrease in the mean decay time.

The frequency responses of the fluorescence intensity decays (Fig. 4) and the relative quantum yields of NB in propylene glycol when quenched by DEA (Fig. 5) were analyzed globally using two models for collisional quenching of fluorescence. In Figs. 4 and 5 the solid lines represent the best global fit using the DDQ model and the dashed lines the best global fit using the RBC model. In all cases, the DDQ model provides an improved fit. The results of frequency-domain and steady-state data analysis of NB quenching using RBC and DDQ models are presented in Table II and III. The global analyses use the same variable parameters at all quencher (DEA) concentrations, which are a, D, and κ for the RBC model and a, r_e, D, and k_a for the DDQ model. During the preliminary analyses we found that simultaneous fitting of all these floating parameters was not possible for either of these models. To be able to proceed with our fitting programs we fixed the distance of the closest approach (a) at several reasonable values. Certain constraints on the parameter κ were also possible. In all RBC-type analyses the parameter κ tended to a very large value, indicating that the data are better described by the pure Smoluchowski model, which implicitly assumes $\kappa = \infty$. Because of this behavior, and also to increase resolution, in further calculations we fixed the parameter κ to a very large value satisfactorily simulating infinity (10^{10} cm/s). Under these conditions, the RBC-type fit for a and D floating resulted

Table II. Global RBC Analysis of Nile Blue Quenching by *N,N*-Diethylaniline in Propylene Glycol (t = 20°C, τ_0 = 1.744 ns)

a (Å)	κ (cm/s)	D (10^{-7} cm²/s)	χ_R^2
⟨5.5⟩[a]	⟨∞⟩[b]	17.1 (16.3–17.9)[c]	108.3
⟨6.5⟩	⟨∞⟩	12.3 (11.8–12.9)	97.3
⟨7.5⟩	⟨∞⟩	8.99 (8.60–9.39)	88.3
⟨8.5⟩	⟨∞⟩	6.65 (6.38–6.95)	81.1
⟨9.5⟩	⟨∞⟩	4.98 (4.77–5.20)	75.4
62.7 (52.7–74.5)	⟨∞⟩	0.005 (0.002–0.009)	53.0

[a]The angular brackets indicate that the parameter was held fixed at the indicated value.
[b]In calculations κ = ∞ has been represented by setting κ = 10^{10} cm/s.
[c]The numbers in parentheses represent the 67% confidence intervals obtained from the least-squares analysis.

Table III. Global DDQ Analysis of Nile Blue Quenching by *N,N*-Diethylaniline in Propylene Glycol (t = 20°C, τ_0 = 1.744 ns)

a (Å)	r_e (Å)	D (10^{-8} cm²/s)	k_a (10^{15} L/s)	χ_R^2
⟨5.5⟩[a]	0.422 (0.411–0.431)[b]	8.59 (7.87–9.24)	110.1 (64.7–171.6)	4.05
⟨6.5⟩	0.407 (0.396–0.415)	8.19 (7.57–8.82)	30.6 (18.7–46.2)	4.06
⟨7.5⟩	0.388 (0.378–0.396)	7.79 (10.0–11.0)	10.3 (6.66–14.9)	4.05
⟨8.5⟩	0.365 (0.355–0.373)	7.25 (6.76–7.72)	4.60 (2.91–6.76)	4.05
⟨9.5⟩	0.342 (0.332–0.350)	6.63 (6.19–7.07)	2.19 (1.34–3.26)	4.06

[a]The angular brackets indicate that the parameter was held fixed at the indicated value.
[b]The numbers in parentheses represent the 67% confidence intervals obtained from the least-squares analysis.

in a nonrealistic value of the distance of the closest approach (a = 62.7 Å; Table II).

A lower limit for the minimum distance (a) can be determined from the size of NB and DEA by considering the van der Waals radii (r_w) of the molecules. An average radius r_w can be obtained from the relation $r_w = (r_x r_y r_z)^{1/3}$,[20] where r_x, r_y, and r_z are the van der Waals radii of the molecule in the x, y, and z direction. For the NB molecule we estimated the r_x, r_y, and r_z values of 6, 3.5, and 1.3 Å, respectively, which give rise to the radius value of r_w = 3.0 Å. Similarly for the DEA molecule we previously calculated[37] r_w = 2.35 Å. Considering the encounter distance as the sum of the van der Waals radii, one could expect the lower limit of the distance to be 5.4 Å. The upper limit of the distance a can be obtained including an intervening solvent molecule. Assuming the diameter of the propylene glycol molecule to be 4 Å, one obtains 9.4 Å for the maximum value of the distance of the NB–DEA closest approach. In further analyses, we used different fixed values of the distance, 5.5, 6.5, 7.5, 8.5, and 9.5 Å. From Figs. 4 and 5 and Table II, it is clearly shown that the RBC model cannot account for the intensity decay of NB quenched by DEA using any encounter distance from 5.5 to 9.5 Å. The deviations between the best-fit RBC model and experimental data points are apparent over the entire frequency range, and are most apparent at the higher frequencies. Similarly, the relative quantum yields obtained from the best global RBC fit do not match the experimental values (Fig. 5). The apparent diffusion coefficient depends strongly on the value of a, suggesting that the model is inadequate. The RBC-predicted values of F_0/F show little upward curvature and do not agree with the measured values. If the encounter distance a is allowed to vary, the recovered value (62.7 Å) is unrealistically large, the recovered diffusion coefficient unrealistically small (Table II), and the value of χ_R^2 is still elevated. These analyses indicate that the RBC model, with a single rate constant for quenching, is not adequate to explain the data for quenching of NB by DEA.

In contrast to the RBC model, the DDQ model was found to be consistent with the experimental data as can be judged by the low values of χ_R^2 (Table III) and good visual agreement between the calculated and the measured frequency-domain decays (Fig. 4) and calculated and measured relative quantum yields (Fig. 5). The Stern–Volmer plots for NB in propylene glycol quenched by DEA at 20°C (see Fig. 5) show significant deviation from linearity and display an upward curvature. The DDQ-determined values of F_0/F are in precise agreement with the measured values. This agreement between two types of experimental data, steady state and frequency domain, provides strong support for a distance-dependent interaction between NB and DEA.

While the DDQ model is able to account for both the time-resolved and the steady-state data, it was not possible to obtain precise values for all four parameters, a, r_e, D, and k_a. The same value of χ_R^2 was obtained for a values ranging from 5.5 to 9.5 Å. Over this range of a values, the values of r_e and D remain relatively constant, but the value of k_a changes dramatically, from 110 to 2 × 10^{15} s^{-1}. However, the apparent change in k_a does

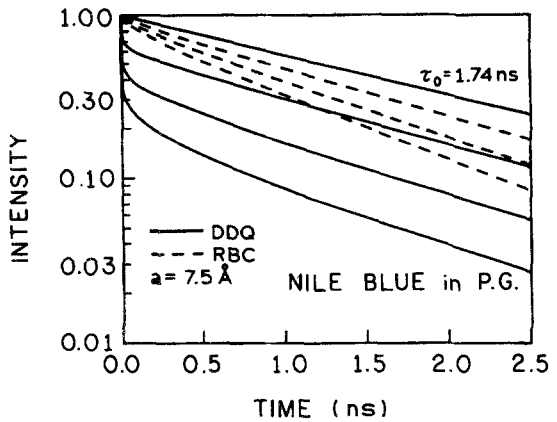

Fig.6. Reconstructed time-dependent intensity decays of Nile Blue in propylene glycol at 20°C quenched by *N,N*-diethylaniline (0, 0.1, 0.2, and 0.3 *M*) for the best-fit DDQ (—) and RBC (- - - -) parameters, using a = 7.5 Å.

not reflect an actual change in the nature of the interaction but, rather, the chosen value of the distance of closest approach (a) and compensation in the apparent value of k_a.

From the best fits to frequency-domain and steady-state data (Figs. 4 and 5), we reconstructed the time-dependent intensity decays of NB in propylene glycol at 20°C (Fig. 6). In the absence of DEA, the intensity decay of NB is a single exponential. The intensity decay becomes nonexponential in the presence of DEA. The effect of the distance-dependent quenching rate is to increase the number of quenchers able to interact at very short times with a given molecule of the fluorophore and, in this way, to create a short-lived component in the decay during the initial 20 ps following excitation. The long-lived component created by the translational diffusion remains comparable in both models for comparable values of the diffusion coefficient. This short-lived component is not allowed by the RBC model (- - -), which consequently is inadequate to explain the frequency-domain data.

It is of interest to compare the diffusion coefficients recovered from the data with those predicted from diffusion theory. The diffusion coefficient of DEA in propylene glycol at 20°C is expected to be $D_Q \approx 1.9 \times 10^{-7}$ cm²/s, as previously calculated[37] based on the Stokes–Einstein equation. Similar calculations carried out for NB result in $D_F \approx 1.5 \times 10^{-7}$ cm²/s. These values of D_Q and D_F yield $D \approx 3.4 \times 10^{-7}$ cm²/s. The RBC model provides values of D (see Table II) which, for reasonable values of parameter a, are larger than the expected value 3.4×10^{-7} cm²/s. This can be understood as an effect of compensation of the lack of the initial drop of the intensity decay by a larger diffusion coefficient so that some additional quenching is introduced even without this rapid drop. However, this compensation in the RBC model is not able to generate the same shape of the fluorescence decay function as that predicted by the DDQ model. The only case when both models can give comparable fits to the data is that characterized by relatively large value of the diffusion coefficient and relatively small values of the parameters k_a and r_e.[32,38] Taking into account the still large value of χ^2_R with a distance of the closest approach of 62.7 Å (Table II), one can see that the RBC model also does not allow a rapid initial drop in the intensity decay, which is needed to fit the experimental data.

The DDQ model results in values of D (Table III) which are several times smaller than the expected value calculated from the Stokes–Einstein equation. Similar results were also observed in our previous papers on the distance-dependent quenching for anthracene quenched by CBr_4,[22] anthracene, and 9,10-dimethylanthracene quenched by DEA[37] and NATA quenched by acrylamide.[23] The explanation of this behavior may be fluorophore–solvent or quencher–solvent interactions, which slow diffusion or increase the size of the diffusing species. The enhanced solvation of the fluorophore and/or quencher molecules may significantly slow down their diffusive motion. Another explanation of the underestimation of the diffusion coefficients in the DDQ model may be that, in reality, the distance dependence of the electron transfer rate constant may be more complex then Eq. (2). The distance dependence of the reorganization energy in the Marcus equation[24–26] may cause the quenching rate not to fall exponentially with fluorophore–quencher distance, but initially to increase with increasing r and then to decrease because the electronic factor, similar to Eq. (2), decreases.[4,39] The possibility of using a full Marcus equation in our data analysis algorithm is now being investigated.

CONCLUSION

The time-resolved and steady-state data reject the RBC model and confirm the distance-dependent rate of quenching [Eq. (2)] for Nile Blue and DEA. Global analysis of the frequency-domain and steady-state data allows for satisfactory resolution of the diffusion coefficient and the two parameters describing the distance-dependent quenching rate, k_a and r_e. This model system can be used for more detailed studies of the effects of solvent polarity and dynamics on the process of electron transfer.

ACKNOWLEDGMENTS

This work was supported by National Institutes of Health Grants GM-39617 and RR-08119, with support for instrumentation from NSF Grant DIR-8710401 and NIH Grant RR-10416.

REFERENCES

1. G. J. Kavarnos (1993) *Fundamentals of Photo-Induced Electron Transfer*, VCH, New York.
2. M. A. Fox and M. Chamon (Eds.) (1988) *Photo-Induced Electron Transfer*, Parts A–D, Elsevier, Amsterdam.
3. J. Mattay (Ed.) in *Topics in Current Chemistry, Vol. 156* (1990), *Vol. 158* (1990), *Vol. 159* (1991), and *Vol. 163* (1992), Springer-Verlag, Berlin/Heidelberg/New York.
4. R. A. Marcus and N. Sutin (1985) *Biochim. Biophys. Acta* **811**, 265–322.
5. J. R. Bolton *et al.* (Eds.) (1991) Electron transfer in inorganic, organic and biological systems, *Advances in Chemistry Series 228*, Am. Chem. Soc., Washington, DC.
6. N. Mataga *et al.* (Eds.) (1992) *Dynamics and Mechanisms of Photo-Induced Electron Transfer and Related Phenomena*, Elsevier, Amsterdam.
7. D. Rehm and A. Weller (1969) *Ber. Bunsenges. Phys. Chem.* **69**, 834–389.
8. D. Rehm and A. Weller (1970) *Israel J. Chem., 21st Farkas Memorial Symp.* **8**, 259–271.
9. P. Suppan (1986) *J. Chem. Soc. Faraday Trans. 1* **82**, 509–511.
10. M. J. Weaver (1992) *Chem. Rev.* **92**, 463–480.
11. G. B. Dutt and N. Periasamy (1991) *J. Chem. Soc. Faraday Trans.* **87**, 3815–3820.
12. H. Heitele (1993) *Angew. Chem. Int. Engl.* **32**, 359–377, and references therein.
13. M. Tachiya (1993) *J. Phys. Chem.* **97**, 5911–5916.
14. T. Asahi, M. Ohkohchi, and N. Mataga (1993) *J. Phys. Chem.* **97**, 13132–13137.
15. Y. Nagasawa, A. P. Yavtsev, K. Tominaga, A. E. Johnson, and K. Yoshikawa (1993) *J. Am. Chem. Soc.* **115**, 7922–7923.
16. K. Yoshikawa, A. Yavtsev, Y. Nagasawa, H. Kandori, A. Donhal, and K. Kemnitz (1993) *Pure Appl. Chem.* **65**, 1671–1675.
17. T. Kobayashi, Y. Takagi, H. Kandori, K. Kemnitz, and K. Yoshikawa (1991) *Chem. Phys. Lett.* **180**, 416–422.
18. H. Kandori, K. Kemnitz, and K. Yoshikawa (1992) *J. Phys. Chem.* **36**, 8042–8048.
19. K. Yoshihara, Y. Nagasawa, A. Yartsev, S. Kumazaki, H. Kandori, A. E. Johnson, and K. Tominaga (1994) *J. Photochem. Photobiol. A Chem.* **80**, 169–175.
20. T. L. Nemzek and W. R. Ware (1975) *J. Chem. Phys.* **62**, 477–489.
21. N. Joshi, M. L. Johnson, I. Gryczynski, and J. R. Lakowicz (1987) *Chem. Phys. Lett.* **135**(3), 200–207.
22. J. R. Lakowicz, J. Kuśba, H. Szmacinski, M. L. Johnson, and I. Gryczynski (1993) *Chem. Phys. Lett.* **206** (5,6), 455–463.
23. J. R. Lakowicz, B. Zelent, I. Gryczynski, J. Kuśba, and M. L. Johnson (1994) *Photochem. Photobiol.* **60**, 205–214.
24. R. A. Marcus (1956) *J. Chem. Phys.* **24**, 966–978.
25. R. A. Marcus (1964) *Annu. Rev. Phys. Chem.* **15**, 155–196.
26. R. A. Marcus (1982) *Faraday Discuss. Chem. Soc.* **74**, 7–15.
27. S. V. Camyshan, N. P. Gritsan, V. V. Korolev, and N. M. Bazhin (1990) *Chem. Phys.* **142**, 59–68.
28. A. Namiki, N. Nakashima, and K. Yoshihara (1979) *J. Chem. Phys.* **71**, 925–930.
29. N. J. Turro (1978) *Modern Molecular Photochemistry*, Benjamin/Cummings, Menlo Park, CA, pp. 305–311.
30. D. D. Eads, B. G. Dismer, and G. R. Fleming (1990) *J. Chem. Phys.* **93**(2), 1136–1148.
31. J. Kuśba and B. Sipp (1988) *Chem. Phys.* **124**, 223–226.
32. J. Kuśba and J. R. Lakowicz (1994) in M. L. Johnson and L. Brand (Eds.), *Methods in Enzymology, Numerical Computer Methods*, Academic Press, New York, Part B, Vol. 240, pp. 216–262.
33. J. Kuśba and B. Sipp (1985) *J. Luminesc.* **33**, 255–260.
34. J. R. Lakowicz, G. Laczko, and I. Gryczynski (1986) *Rev. Sci. Instrum.* **57**, 2499–2506.
35. G. Laczko, I. Gryczynski, Z. Gryczynski, W. Wiczk, H. Malak, and J. R. Lakowicz (1990) *Rev. Sci. Instrum.* **61**, 2331–2337.
36. G. Briegleb and J. Czekalla (1959) *Z. Elektrochem.* **63**, 6–12.
37. B. Zelent, J. Kuśba, I. Gryczynski, and J. R. Lakowicz (1995) *Appl. Spectrosc.* **49**, 43–50.
38. J. Kuśba, I. Gryczynski, H. Szmacinski, M. L. Johnson, and J. R. Lakowicz (1992) *SPIE* **1640**, 46–57.
39. M. Tachiya and S. Murata (1992) *J. Phys. Chem.* **96**, 8441–8444.